Frontiers in Bioscience Landmark

Front. Biosci. (Landmark Ed) **2023**; 28(5): 102
https://doi.org/10.31083/j.fbl2805102

Original Research

rRNA-Derived Small RNA rsRNA-28S Regulates the Chemoresistance of Prostate Cancer Cells by Targeting PTGIS

Deqian Qiao[1,2,†], Yiling Liu[1,2,†], Yunlong Lei[1,2], Chundong Zhang[1,2], Youquan Bu[1,2], Yishu Tang[3,*], Ying Zhang[1,2,*]

[1]Department of Biochemistry and Molecular Biology, School of Basic Medicine, Chongqing Medical University, 400016 Chongqing, China
[2]Molecular Medicine and Cancer Research Center, Chongqing Medical University, 400016 Chongqing, China
[3]Department of Laboratory Medicine, The First Affiliated Hospital of Chongqing Medical University, 400016 Chongqing, China
*Correspondence: tangyishu@cqmu.edu.cn (Yishu Tang); zhangying@cqmu.edu.cn (Ying Zhang)
[†]These authors contributed equally.
Academic Editor: Amancio Carnero Moya
Submitted: 24 February 2023 Revised: 7 April 2023 Accepted: 10 April 2023 Published: 25 May 2023

Abstract

Background: rRNA-derived small RNAs (rsRNAs) represent a novel class of small non-coding RNAs (sncRNAs), produced by the specific cleavage of rRNAs; however, their roles in tumor development are unclear. In the present study, we explored the effect of a kind of rsRNA-28S, which originates from 28S rRNA, on the chemoresistance of prostate cancer cells and the mechanisms underlying its effect. **Methods**: Quantitative reverse transcription PCR (RT-PCR) was performed to quantify rsRNA-28S levels in serum samples taken from prostate cancer patients. DU-145R cells, which are resistant to both paclitaxel and docetaxel, were generated from parental DU-145 cells. Northern blot was conducted to detect cellular rsRNA-28S levels following drug treatments. To verify the effect of rsRNAs-28S on chemoresistance, antisense oligonucleotides were utilized to block rsRNA-28S functions, and a series of assays were further performed, such as cell viability, cell proliferation, colony formation and tumor sphere formation. The target gene of rsRNA-28S was explored using dual-luciferase reporter gene assay. **Results**: The rsRNA-28S level was reduced in the serum samples of patients who received chemotherapy compared to that of patients who did not. Furthermore, the rsRNA-28S level was remarkably declined in DU-145R cells, and drug treatments decreased the levels of rsRNA-28S in DU-145 and DU-145R cells. Moreover, rsRNA-28S inhibition enhanced the chemoresistance of prostate cancer cells as well as their cancer stem cell characteristics. Mechanistically, the prostaglandin I2 synthase (*PTGIS*) gene transcript was verified as a target of rsRNA-28S, as rsRNA-28S inhibited the translation of PTGIS mRNA by directly binding the 3′ untranslated region of PTGIS mRNA. rsRNA-28S inhibition was also found to increase PTGIS abundance, and PTGIS overexpression significantly enhanced prostate cancer cell chemoresistance. **Conclusions**: Our findings indicate that rsRNA-28S attenuates prostate cancer cell chemoresistance by downregulating its target gene *PTGIS*. This study not only greatly contributes to systematic identification and functional elucidation of chemoresistance relevant rsRNAs, but also promotes rsRNA-included combinatorial therapeutic regimens for cancer.

Keywords: prostate cancer; chemoresistance; sncRNA; rsRNA; PTGIS

1. Introduction

Cancer is the leading cause of death in China and places a major economic burden on the nation's public health system. Over the past three decades, the cancer spectrum of China shifted towards that of developed countries, with the incidence and mortality rates of lung cancer, breast cancer, colorectal cancer, and prostate cancer increasing at a fast rate [1,2]. Prostate cancer ranks as the sixth most common cancer in men, and based on estimates from National Cancer Center of China, approximately 78,300 new cases (11.05 per 100,000) and 33,600 deaths (4.75 per 100,000) from prostate cancer occurred in China in 2016 [3,4]. The five-year survival rate for patients with non-metastatic prostate cancer is 98.9%, while patients with metastatic prostate cancer show a dismal 28.2% of five-year survival rate [5]. Castration-induced androgen deprivation therapy (ADT) is the first-line suggested therapy for hormone-dependent prostate cancer with metastases; however, almost all patients will progress to castration resistance after two years of treatment [6]. Paclitaxel (PTX) and docetaxel (DOC) are principal chemotherapeutic drugs for metastatic castration-resistant prostate cancer (mCRPC) and effectively improve patient survival [7–10]. Unfortunately, these therapeutics often drive cancer cell chemoresistance [11]. Therefore, a better understanding of the molecular mechanisms underlying prostate cancer chemoresistance is beneficial to develop new therapeutic regimens for mCRPC treatment.

Ribosomal RNAs (rRNAs) are the most abundant RNA transcripts in eukaryotic cells. rRNAs, along with ribosomal proteins, assemble into ribosomes that are required for protein translation. In eukaryotes, ribosomes contain four rRNA transcripts, specifically, 5S, 5.8S, 18S and 28S, and approximately 80 ribosomal proteins. Within the ri-

bosome, rRNAs form highly conserved secondary structures that complex with ribosomal proteins as well as recognize motifs within transfer RNAs (tRNAs) and messenger RNAs (mRNAs). In recent years, pilot studies have uncovered a novel class of small non-coding RNAs (sncRNAs), produced by the specific cleavage of rRNAs. Accordingly, this class of sncRNAs is termed rRNA-derived small RNAs (rsRNAs) and are viewed as one of the most ancient classes of sncRNAs that emerged with the advent of rRNAs [12,13]. Studies on rsRNAs have to date largely focused on spermatogenesis, where rsRNAs have been implicated in sperm quality and male fertility [14–17]. Similar to tRNA-derived small RNAs (tsRNAs), rsRNAs also constitute the sperm RNA code, transmitting traits to zygotes and impacting early embryonic development [12,18]. Potential roles for rsRNAs in tumorigenesis has not been extensively explored with a single study, which documented that a kind of rsRNA-28S promoted cellular proliferation but inhibited apoptosis of non-small cell lung cancer cells [19]. Recently, a "disease RNA code", which combines rsRNAs, tsRNAs, and yRNA-derived small RNAs (ysRNAs), was harnessed in lung cancer screening [20], indicating its promising application as diagnostic markers and/or therapeutic targets in cancer [12].

We previously engaged in the development of a novel sncRNA sequencing method, namely PANDORA-seq, that revealed unprecedented landscapes of tsRNAs, rsRNAs and ysRNAs. Using this discovery platform, an abundant 37-nt rsRNA was identified stemming from the 5′ end of 28S rRNA (referred to as "rsRNA-28S") (**Supplementary Fig. 1**). This rsRNA-28S, termed rsRNA-28S, prompted mouse embryonic stem cell (ESC) differentiation and downregulated cellular translational efficiency [21]. Given that tumors generally display dedifferentiation and enhanced translational efficiency, we hypothesized that rsRNA-28S is likely to play a vital role in tumorigenesis.

Herein, we present the first evidence that rsRNA-28S impacts prostate cancer cell chemoresistance by targeting the prostaglandin I2 synthase (PTGIS) gene transcript. This seminal work not only greatly contributes to subsequent systematic identification and functional elucidation of chemoresistance relevant rsRNAs, but also provide needed information for therapeutic approaches to target rsRNAs in mCRPC treatment.

2. Materials and Methods

2.1 Clinical Serum Samples

This study was approved by the Ethics Committee of The First Affiliated Hospital of Chongqing Medical University and informed consent was obtained from all subjects involved in the study. Blood samples were collected from 23 prostate cancer patients, including 13 cases who received chemotherapy (PTX or DOC) and 10 cases who didn't receive chemotherapy prior to blood sampling. Whole blood samples were collected in EDTA-containing tubes, and the tubes were subsequently incubated at room temperature for 15 minutes followed by centrifugation at 5000 g for 10 minutes. To remove residual cells and debris, the supernatant was transferred to new tubes and further centrifuged at 16,000 g for 15 minutes. Finally, clear serum samples were divided into aliquots and stored at –80 °C until further processing. The clinicopathological characteristics of enrolled patients are summarized in **Supplementary Table 1**.

2.2 Cell Culture

The androgen-negative human prostate cancer cell line DU-145 was purchased from Kunming Cell Bank of Type Culture Collection (Kunming, China). The cell line has been authenticated by short tandem repeat, and mycoplasma testing has been done. Cells were cultured in RPMI 1640 medium (Hyclone, Logan, UT, USA) supplemented with 10% fetal bovine serum (ExCell Bio, Shanghai, China), streptomycin (100 μg/mL) and penicillin (100 IU/mL). All cells were maintained in a 5% CO_2 humidified incubator at 37 °C.

2.3 Establishment of PTX-Resistant Cells

PTX-resistant DU-145 cells, designated DU-145R, were generated from the parental DU-145 cell line following a drug dose escalation strategy [22]. Briefly, DU-145 cells were initially cultured in medium containing 5 nM PTX (Aladdin, Shanghai, China). After removing dead cells, the surviving cells were restored to exponential growth in the medium without PTX. Thereafter, cells were cultured in the medium with a 100% increased concentration of PTX. This procedure was repeated until the PTX-resistant phenotype was developed, with a tolerance of 160 nM PTX.

2.4 Cell Transfection

To inhibit rsRNA-28S, an antisense oligonucleotide (ASO) targeting rsRNA-28S, denoted as rsRNA-28S ASO, and a negative control ASO, denoted as NC ASO, were designed and synthesized by Genepharma (Shanghai, China). Chimeric ASOs were designed to be complementary phosphorothioate-modified DNA sequences flanked by 2′OMe modified RNA. The sequences of both rsRNA-28S ASO and NC ASO are listed in **Supplementary Table 2**. Cells were transiently transfected with rsRNA-28S ASO or NC ASO at a final concentration of 40 nM using Lipofectamine™ RNAiMAX reagent (Invitrogen, Carlsbad, CA, USA) according to the manufacturer's instructions.

For overexpression of PTGIS, a full-length PTGIS expression plasmid was donated by Prof Xinghuan Wang (Department of Urology, Zhongnan Hospital of Wuhan University) [23]. Cells were transiently transfected with the PTGIS plasmid or empty pcDNA3.0 vector (Invitrogen, CA, USA) using Lipofectamine 3000 (Invitrogen, CA, USA) according to the manufacturer's instructions.

2.5 Cell Viability Assay

Cells were seeded in 96-well plates at a density of 3000 cells per well followed by treatments with indicated concentrations of PTX or DOC (Meilunbio, Dalian, China) for 24 h. Cytotoxicity assay was determined by Cell Counting Kit-8 (CCK-8) (Bimake, Houston, TX, USA), according to the manufacturer's instructions. The viable cells at each time point were recorded as absorbance at 450 nm. Three independent experiments were performed, each in triplicate.

2.6 Cell Proliferation Assay

Cells were seeded in 96-well plates at a density of 1000 cells per well. Cell proliferation was measured by CCK-8 (Bimake, TX, USA), according to the manufacturer's instructions. The viable cells at each time point were recorded as absorbance at 450 nm. Three independent experiments were performed, each in triplicate.

2.7 Colony Formation Assay

Cells were seeded in 6-well plates at a density of 1000 cells per well with complete medium and cultured for approximately 14 days. Subsequently, cells were sequentially washed twice with PBS, fixed with methanol for 30 min, stained with 0.1% crystal violet solution for 30 min, and washed three times with PBS prior to obtaining images. Three independent experiments were performed, each in triplicate.

2.8 Tumor-Sphere Formation Assay

Cells were cultured at a density of 3000 per well in 6-well, ultra-low attachment plates (Corning, Corning, NY, USA) with stem cell medium, specifically, RPMI 1640 medium supplemented with 20 ng/mL epidermal growth factor (EGF, Sino Biological, Beijing, China), 20 ng/mL basic fibroblast growth factor (bFGF, Sino Biological, Houston, TX, USA), 2% B27 (Invitrogen, CA, USA), streptomycin (100 μg/mL) and penicillin (100 IU/mL). Half the volume of medium was replaced with fresh stem cell medium every 3 days. Following approximately a one-week incubation, the numbers of tumor-spheres with a diameter greater than 100 μm were counted. Three independent experiments were performed, each in triplicate.

2.9 Dual-Luciferase Reporter Gene Assay

cDNA corresponding to the 3′ untranslated region (3′UTR) of the PTGIS mRNA sequence containing either a wild-type or mutant rsRNA-28S binding site was subcloned into pmiRGLO vector (Tsingke, Beijing, China). Cells were seeded at a density of 5×10^4 cells per well in 24-well plates and then co-transfected with the indicated reporter plasmids and rsRNA-28S ASO or NC ASO using Lipofectamine 3000 (Invitrogen, CA, USA). After transfection for 24 h, both Firefly and Renilla luciferase activities were determined using Dual-Luciferase Reporter Assay System (Beyotime, Shanghai, China) according to the manufacturer's instructions. Three independent experiments were performed, each in triplicate.

2.10 RNA Isolation and Quantitative RT-PCR

Total RNA was extracted from serum samples using TRIzol LS reagent (Invitrogen, CA, USA) according to the manufacturer's instructions. Total RNA was extracted from cells using TRIzol reagent (Invitrogen, CA, USA), following the manufacturer's instructions. For rsRNA-28S detection, cDNA was synthesized from 500 ng of total RNA using the PrimeScript™ II 1st Strand cDNA synthesis Kit (Takara, Tokyo, Japan) following the manufacturer's instructions. For PTGIS mRNA detection, the cDNA was synthesized from 500 ng of total RNA using the PrimeScript™ RT Master Mix Kit (Takara, Tokyo, Japan) following the manufacturer's instructions. Quantitative real-time PCR was performed using the SYBR Kit (Bimake, TX, USA). The $2^{-\Delta\Delta Ct}$ method was used to calculate the relative abundance of rsRNA-28S and indicated target genes, with U6 and GAPDH transcripts as the loading controls, respectively. The sequences of the primers used for RT-PCR are listed in **Supplementary Table 2**.

2.11 Northern Blot

Total RNA was extracted from cells using TRIzol reagent (Invitrogen, CA, USA) according to the manufacturer's instructions. RNA samples were separated on a 10% PAGE gel containing urea and subsequently stained with SYBR Gold. The gel contents were transferred to positively charged nylon membranes (Roche, Basel, Switzerland) and transferred nucleic acids were crosslinked to the membrane with 0.12 J ultraviolet radiation. After pre-hybridization with DIG Easy Hyb solution (Roche, Basel, Switzerland) for 1 h at 42 °C, the membrane was incubated overnight at 42 °C with the DIG-labelled rsRNA-28S probe (Sangon Biotech, Shanghai, China). Following this, the membrane was washed, blocked for 3 h, and then incubated with anti-Dig-AP antibody (11093274910, Roche, Basel, Switzerland) for 30 min. Finally, the RNA signal was detected using chemiluminescenece substrate CSPD (Roche, Basel, Switzerland) and ChemiDoc™ Imaging System (Bio-Rad, Hercules, CA, USA).

2.12 Western Blot

The Western blot procedure used in this study has been previously described in detail [24]. The primary antibodies included rabbit monoclonal anti-CD44 (1:1000) (60224-1-Ig, Proteintech, IL, USA), rabbit monoclonal anti-ABCG2 (1:500) (27286-1-AP, Proteintech, Chicago, IL, USA), Rabbit monoclonal anti-PTGIS (1:1000) (ab23668, Abcam, Cambridge, UK), rabbit polyclonal anti-β-actin (1:1000) (4970, Cell Signaling Technology, Boston, MA, USA).

2.13 Statistical Analysis

Statistical analyses were conducted using SPSS software, version 22.0 (SPSS Inc., Chicago, IL, USA). Comparisons between two groups were performed using two-tailed independent Student's *t*-test, and *p* values of <0.05 were interpreted statistically significant. In addition, the secondary structure of rsRNA-28S (sequence: CGCGACCTCAGATCAGACGTGGCGACCCGCTGAATTT) was predicted via RNAfold web server (http://rna.tbi.univie.ac.at/cgi-bin/RNAWebSuite/RNAfold.cgi) [25]. The potential targets of rsRNA-28S were predicted via the TargetRank web server (http://hollywood.mit.edu/targetrank/) [26].

3. Results

3.1 The rsRNA-28S Level is Decreased in the Serum Samples of Prostate Cancer Patients Receiving Chemotherapy

To explore the potential clinical significance of rsRNA-28S in prostate cancer, quantitative RT-PCR was performed to quantify the rsRNA-28S level in serum samples taken from prostate cancer patients. The results showed that the rsRNA-28S level was reduced in patients who received chemotherapy compared to those who did not receive chemotherapy; however, the reduction was not significantly ($p = 0.352$, Fig. 1A). In addition, the rsRNA-28S level was increased in patients with poorly differentiated prostate cancer relative to those with more moderately differentiated cancer ($p = 0.0197$, Fig. 1B). These results suggest a potential association between rsRNA-28S and biological behavior of prostate cancer.

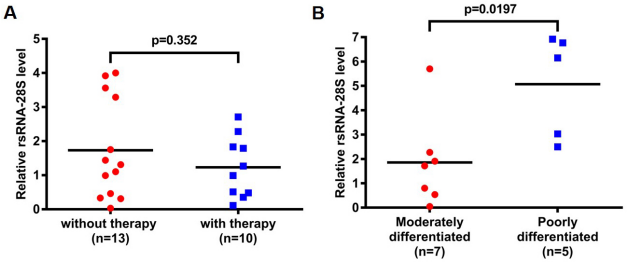

Fig. 1. Relative rsRNA-28S levels in serum samples from prostate cancer patients treated with or without chemotherapy. (A) Relative rsRNA-28S levels in the serum samples obtained from prostate cancer patients with or without chemotherapy were measured using quantitative RT-PCR. (B) Relative rsRNA-28S levels in the serum samples obtained from prostate cancer patients with different differentiation status was measured using quantitative RT-PCR. The U6 transcript served as the loading control. Data are displayed using scatter plots and mean values are represented by horizontal lines.

3.2 The rsRNA-28S Level is Decreased in DU-145R Cells

To confirm the sensitivity of DU-145 and DU-145R cells to PTX and DOC, CCK-8 assay was conducted to examine cell viability rates after various doses of drug. The cell viability of DU-145 cells notably declined with increasing concentrations of PTX or DOC. Specifically, DU-145 IC50 values for PTX and DOC were 20 nM and 250 nM, respectively. In contrast, neither PTX nor DOC could measurably decrease the cell viability rate of DU-145R cells at the outlined doses (Fig. 2A,B). These results indicate that DU-145 cells are sensitive to PTX and DOC, whereas DU-145R cells are resistant to these chemotherapeutic drugs at the same dose.

Taking the relevance of chemoresistance with the characteristics of cancer stem cells (CSC) into consideration [27], we further tested the self-renewal capacities of DU-145 and DU-145R cells using tumor-sphere formation assay. Data obtained indicate that DU-145R cells gave rise to more and larger tumor-spheres than DU-145 cells ($p = 0.036$, Fig. 2C,D). In line with this data, the levels of two key CSC markers, CD44 and ABCG2, were remarkably higher in DU-145R cells than that observed in the parental DU-145 cell line (Fig. 2E). Additionally, we also found that the proliferative capability of DU-145R cells is weaker than that of DU-145 cells (**Supplementary Fig. 2**). These results indicate that DU-145R cells harbor greater CSC characteristics consistent with their chemoresistant phenotype.

Next, we examined rsRNA-28S levels in DU-145 and DU-145R cells using Northern blot and quantitative RT-PCR. In comparison to DU-145 cells, the rsRNA-28S abundance was substantially reduced in DU-145R cells (Fig. 2G,I and **Supplementary Fig. 3**). After treatment with PTX or DOC (Fig. 2F,H), rsRNA-28S levels were downregulated in both DU-145 and DU-145R cells (Fig. 2G,I). These results imply that rsRNA-28S may attenuate the chemoresistance of prostate cancer cells.

3.3 rsRNA-28S Inhibition Enhances Chemoresistance of DU-145 and DU-145R Cells

To understand the effect of rsRNA-28S on the chemoresistance of prostate cancer cells, functional studies were performed by blocking rsRNA-28S function using antisense oligonucleotides (ASOs) in both DU-145 and DU-145R cells (Fig. 3A and **Supplementary Fig. 4**). Transfection of rsRNA-28S ASO led to a dramatic increase in cell viability rates of both DU-145 and DU-145R cells after either PTX or DOC treatment (Fig. 3C–F). Meanwhile, ABCG2 and CD44 were upregulated following ASO-mediated inhibition of rsRNA-28S in either DU-145 or DU-145R cells (Fig. 3B). We also found that rsRNA-28S ASO significantly reduced the proliferative capability of both cell lines (**Supplementary Fig. 5**). These results suggest that rsRNA-28S recede the chemoresistance of prostate cancer cells.

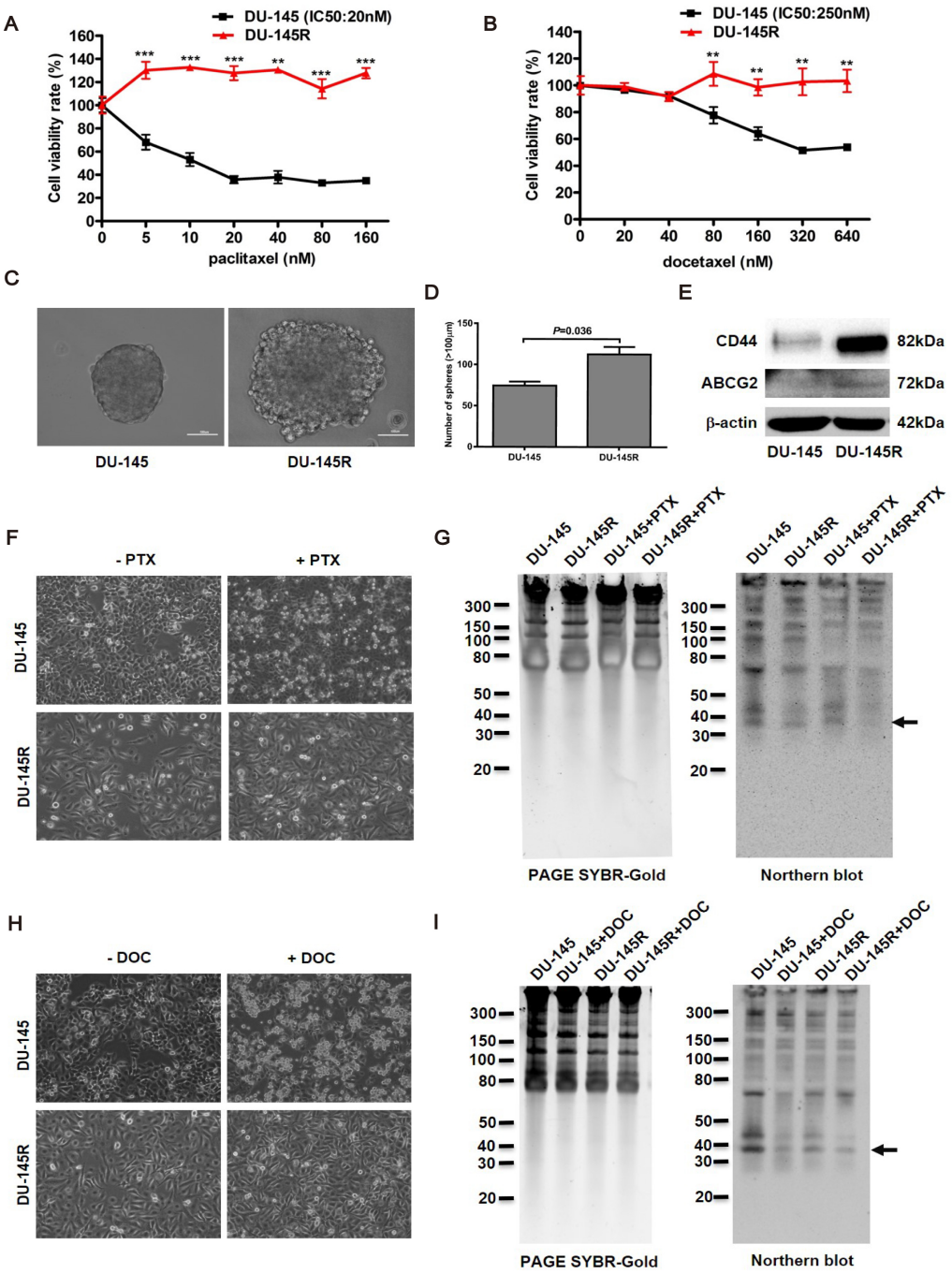

Fig. 2. DU-145R cells display differential rsRNA-28S expression when compared to the parental DU-145 cell line. (A,B) Cell viabilities of DU-145 and DU-145R cells treated with the indicated concentrations of PTX (A) or DOC (B) were measured using CCK-8 assay. Three independent experiments were performed in triplicate, and data are shown as the mean ± SD (two-sided independent Student's *t*-test, $^{**}p < 0.01$, and $^{***}p < 0.001$). (C) Representative microscopic views of tumor-spheres formed in cultures of DU-145 and DU-145R cells (200× magnification). Scale bar = 100 μm. (D) Number of tumor-spheres with a diameter larger than 100 μm formed by DU-145 and DU-145R cells in each well. Mean ± SD (two-sided independent Student's *t*-test) is shown from three independent experiments conducted in triplicate. (E) The expression levels of CD44 and ABCG2 in DU-145 and DU-145R cells were determined using Western blot, with β-actin as the loading control. (F) Representative microscopic views of DU-145 and DU-145R cells treated with the IC50 dose of PTX were photographed (100× magnification). (G) The expression levels of rsRNA-28S in DU-145 and DU-145R cells treated with the IC50 dose of PTX were detected using Northern blot. (H) Representative microscopic views of DU-145 and DU-145R cells treated with the IC50 dose of DOC were photographed (100× magnification). (I) The expression levels of rsRNA-28S in DU-145 and DU-145R cells treated with the IC50 dose of DOC were detected using Northern Blot.

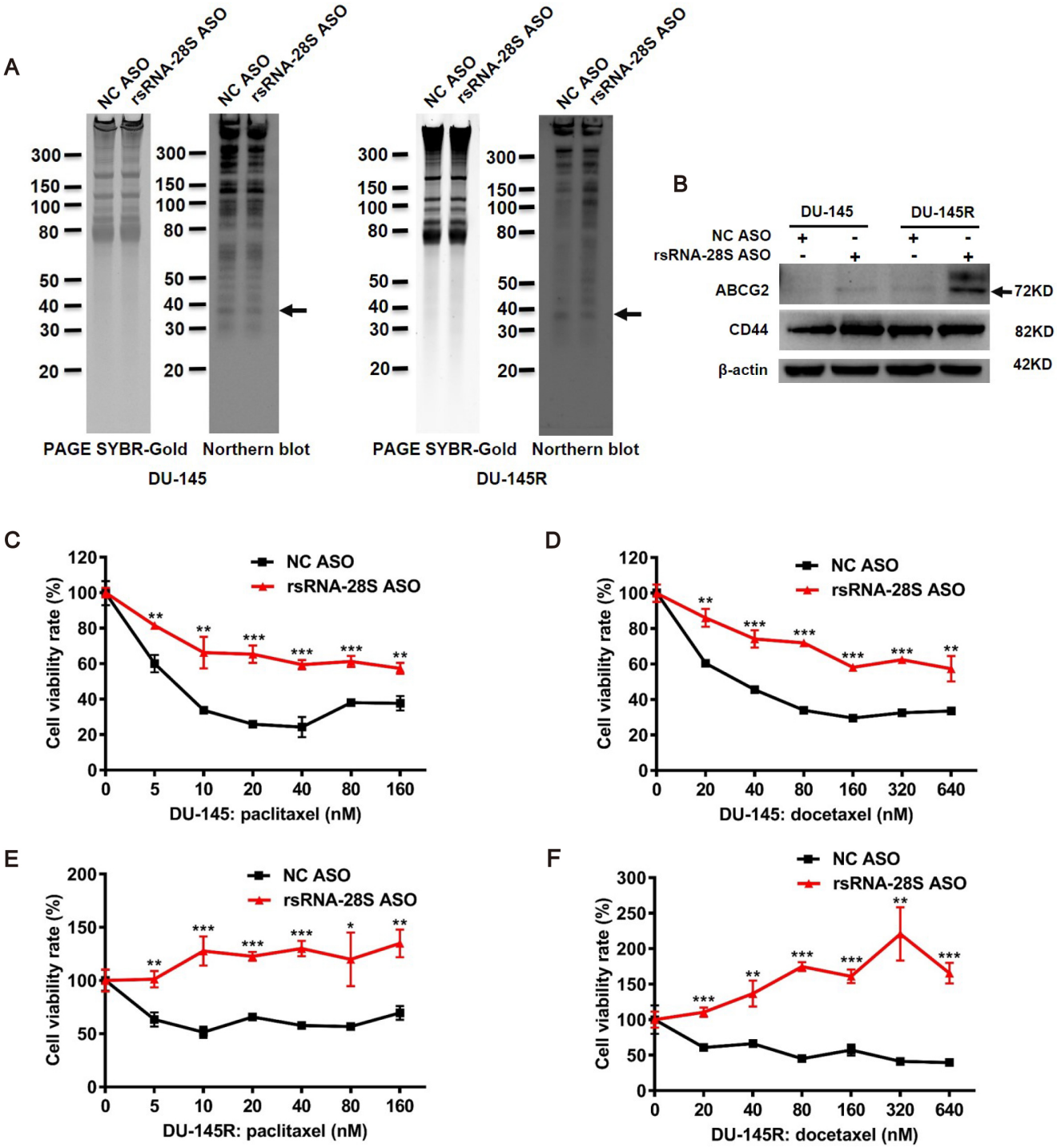

Fig. 3. rsRNA-28S ASO enhances the chemoresistance of DU-145 and DU-145R cells. (A) rsRNA-28S levels in DU-145 and DU-145R cells transfected with rsRNA-28S ASO were detected using Northern blot. (B) Levels of CD44 and ABCG2 in DU-145 and DU-145R cells transfected with rsRNA-28S ASO were determined using Western blot, with β-actin as the loading control. (C,D) Cell viability of DU-145 cells transfected with rsRNA-28S ASO followed by treatment with the indicated concentrations of PTX (C) or DOC (D) was measured using CCK-8 assay. (E,F) Cell viability of DU-145R cells transfected with rsRNA-28S ASO followed by treatment with the indicated concentrations of PTX (E) or DOC (F) was measured using CCK-8 assay. Three independent experiments were performed in triplicate, and data are shown as the mean $\pm$ SD (two-sided independent Student's *t*-test, $^{*}p < 0.05$, $^{**}p < 0.01$, and $^{***}p < 0.001$).

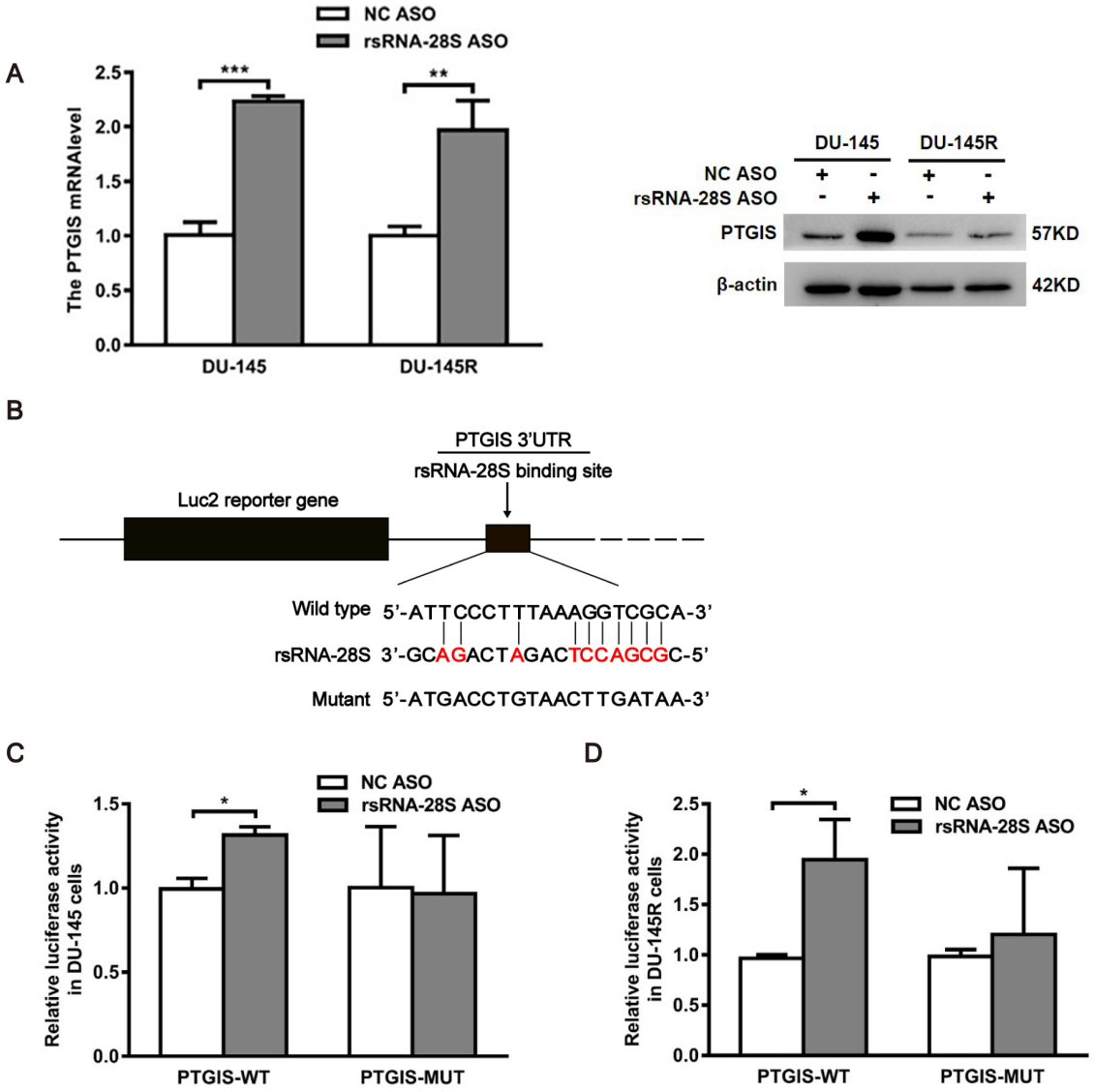

Fig. 4. rsRNA-28S directly mediates PTGIS expression in DU-145 and DU-145R cells. (A) The expression levels of PTGIS in DU-145 and DU-145R cells transiently transfected with rsRNA-28S ASO were measured using quantitative RT-PCR (*left*) and Western Blot (*right*). GAPDH and β-actin served as the loading control, respectively. (B) A schematic of the PTGIS 3′UTR and predicted binding site for rsRNA-28S is shown. Wild-type and mutant 3′UTR sequences are provided. (C,D) Luciferase constructs containing either the wild-type or mutant PTGIS 3′UTR were transfected into DU-145 (C) and DU-145R (D) cells along with either rsRNA-28S ASO or NC ASO as indicated. Data are shown as mean $\pm$ SD (Two-sided independent Student's *t*-test, $*p < 0.05$, $**p < 0.01$, $***p < 0.001$).

3.4 PTGIS is a Potential Target of rsRNA-28S

Recent studies have underscored the functionality of rsRNAs in a miRNA-like manner [28]. To explore the mechanism underlying the effect of rsRNA-28S on chemoresistance, we examined a list of predicted targets of rsRNA-28S using TargetRank database. The PTGIS transcript was selected for further analysis based on literature mining (**Supplementary Table 3**). The results of quantitative RT-PCR and Western blot displayed that the PTGIS levels were remarkably upregulated in DU-145 and DU-145R cells following transfection with rsRNA-28S ASO (Fig. 4). Sequence inspection revealed that the 3′UTR of the PTGIS transcript embraced a potential binding site for rsRNA-28S. Luciferase-reporter plasmids containing sequences corresponding to either wild-type or mutant PTGIS 3′UTR were constructed (Fig. 4). Subsequently, these wild-type or mutant constructs were co-transfected along with either rsRNA-28S ASO or NC ASO into DU-145 and DU-145R cells. As shown in Fig. 4C,D, rsRNA-28S ASO significantly increased relative luciferase activity when co-transfected along with the wild-type reporter plasmid. In contrast, rsRNA-28S ASO had no effect on the relative luciferase activity of the mutant reporter plasmid. These results clearly suggest that rsRNA-28S can inhibit the translation of the PTGIS mRNA by directly targeting its 3′UTR.

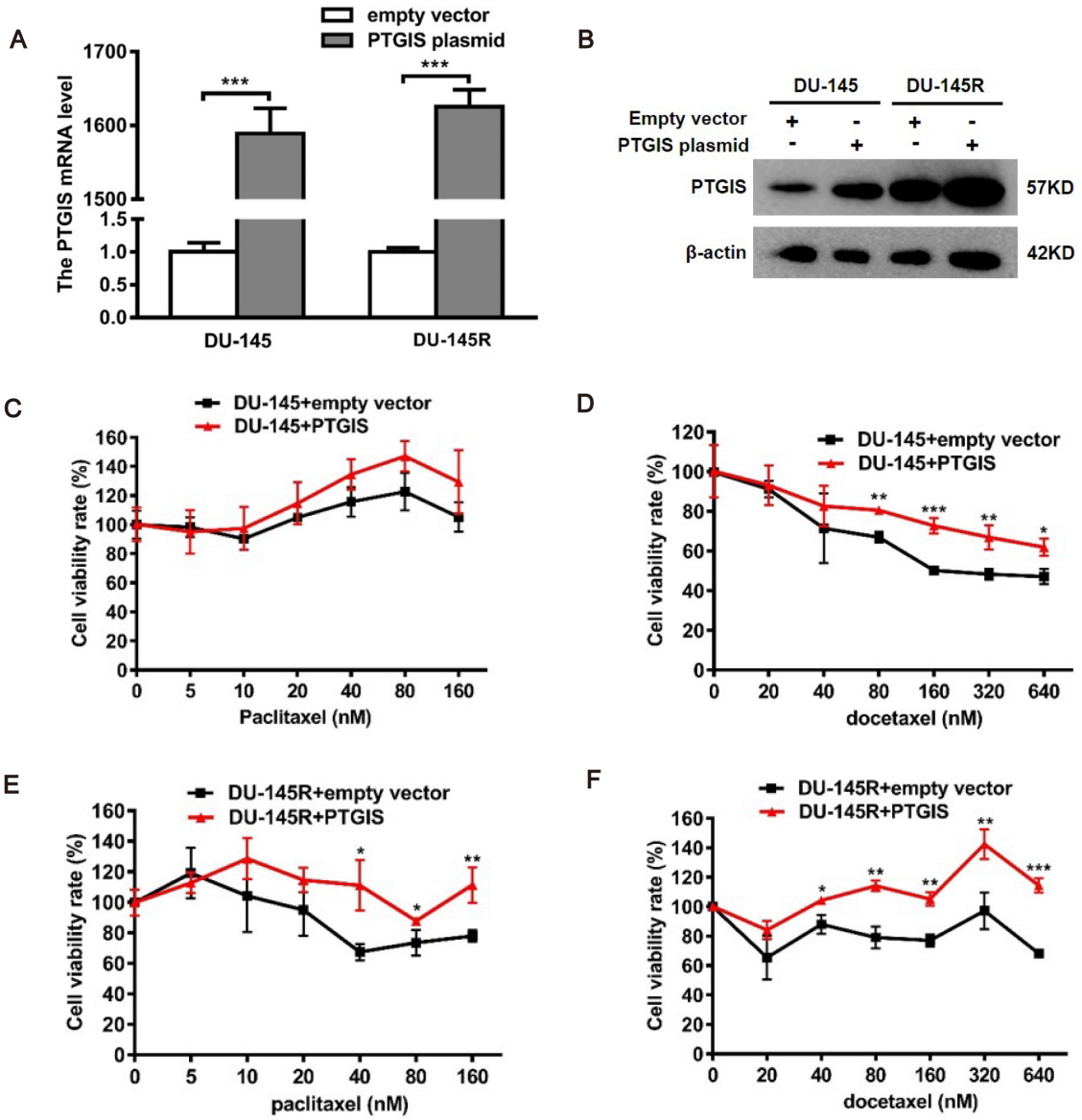

Fig. 5. PTGIS overexpression enhances the chemoresistance of DU-145 and DU-145R cells. (A,B) Expression levels of PTGIS in DU-145 and DU-145R cells transiently transfected with a PTGIS expression plasmid were detected using quantitative RT-PCR (A) and Western blot (B). GAPDH and β-actin served as the loading control, respectively. (C,D) Cell viability of DU-145 cells transiently transfected with the PTGIS expression plasmid followed by treatment with the indicated concentrations of PTX (C) or DOC (D) was measured using CCK-8 assay. (E,F) Cell viability of DU-145R cells transiently transfected with a PTGIS expression plasmid followed by treatment with the indicated concentrations of PTX (E) or DOC (F) was measured using CCK-8 assay. Three independent experiments were performed in triplicate, and data are shown as mean $\pm$ SD (two-sided independent Student's *t*-test, $^{*}p < 0.05$, $^{**}p < 0.01$, and $^{***}p < 0.001$).

3.5 PTGIS Overexpression Enhances the Chemoresistance of DU-145 and DU-145R Cells

Given that rsRNA-28S attenuates the chemoresistance of prostate cancer cells, and PTGIS is a potential target of rsRNA-28S, we further tested the effect of PTGIS on chemoresistance in prostate cancer cells. DU-145 and DU-145R cells were transiently transfected with a full-length PTGIS expression plasmid (Fig. 5A,B) followed by treatment with PTX or DOC. Similar to the effect noted with rsRNA-28S ASO, PTGIS overexpression markedly increased the cell viability rates of DU-145 and DU-145R cells after PTX or DOC treatment (Fig. 5C–F). In addition, PTGIS overexpression didn't appreciably affect the proliferative capability of either DU-145 or DU-145R cells (**Supplementary Fig. 6**). Taken together, these results suggest that rsRNA-28S likely attenuates the chemoresistance of prostate cancer cells, at least in part, by downregulating its downstream target PTGIS.

4. Discussion

rsRNAs represent a novel class of sncRNAs and interest in their systematic identification and functional elucidation has become an emerging frontier in life sciences. Next-generation RNA sequencing is optimal for the detection of sncRNAs in high-throughput; however, the traditional construction of cDNA libraries for small RNA-seq is not suitable for rsRNAs. rsRNAs harbor terminal modifications such as 5′-hydroxyl (5′-OH), 3′-phosphate (3′-P), and 2′,3′-cyclic phosphate (2′,3′-cP). Such modifications are not compatible with adaptor ligation, which depends on the presence of 5′-P and 3′-OH moieties on RNA molecules [13,21]. Further, rsRNAs commonly harbor internal modifications, such as methylation patterns inherited from rRNAs, and these modifications prevent the process of reverse transcription [13,21]. Based on these considerations, it is challenging to catalog the full spectrum of rsRNAs using conventional RNA-seq, since the complete cDNA libraries of rsRNAs can't be generated via the traditional small RNA-seq process. To overcome this technical hurdle, investigators have proposed enzymatic methods to uncover modified sncRNAs using RNA-seq. We participated in the development of PANDORA-seq. This approach improves both adaptor ligation and reverse transcription based on combinatorial enzymatic treatments of T4PNK and AlkB. Therefore, PANDORA-seq can provide comprehensive identification of sncRNAs, including miRNA, piRNA, tsRNA, rsRNA and ysRNA [21]. Using PANDORA-seq, the expression profiles of sncRNAs were determined in six tissue/cell types in mice (brain, liver, spleen, ESC, sperm, and sperm heads) and three cell types in humans (primed mESCs, naïve ESCs, and Hela cells). From these efforts we noted that rsRNAs are much more abundant than other sncRNA species [21], highly reminiscent of their evolutionarily conserved functions.

As the most abundant form of rsRNAs, rsRNA-28S mainly stems from the 5′ or 3′ end of 28S rRNAs. The functions of rsRNA-28S largely depend on its sequence, modifications and/or structure [28]. In previous work using PANDORA-seq, a kind of 37-nt 2rsRNA-28S was identified from the 5′ end of 28S rRNA, and was verified to promote mouse ESC differentiation by downregulating cellular translational efficiency [21]. As tumors generally exhibit the characteristics of dedifferentiation and enhanced translational efficiency. This leads us to explore the potential effects of rsRNA-28S on tumor cell phenotyes, particularly on cell chemoresistance.

In the present study, PTX and DOC-resistant DU-145R cells were generated from parental DU-145 cells. The rsRNA-28S level was decreased in DU-145R cells, and both PTX and DOC treatments downregulated the rsRNA-28S levels in DU-145 and DU-145R cells (Fig. 2). Furthermore, rsRNA-28S inhibition enhanced chemoresistance of DU-145 and DU-145R cells as well as their CSC characteristics (Fig. 3). These results suggested that rsRNA-28S may attenuate the chemoresistance of prostate cancer cells via receding their CSC characteristics. Of note, the effect of rsRNA-28S on CSC characteristics was consistent with the previous finding that rsRNA-28S promoted mouse ESC differentiation [21].

While rsRNA-28S function has received little attention in cancer research, accumulating evidence has revealed that rsRNA-28S is implicated in sperm quality and male fertility. The diminished rsRNA-28S in semen samples from leukocytospermia patients implied its relevance to the subfertility observed in leukocytospermia patients [14]. Sperm samples from which low-quality embryos were produced *in vitro* contained reduced levels of rsRNA-28S [17]. Natt and Ost proposed that sperm sncRNAs display dynamic changes during various stages of spermatogenesis. piRNAs and miRNAs dominate in early stages of development, while tsRNAs and rsRNAs overwhelm in late developmental stages [16]. They also discovered that the majority of sncRNAs isolated in ejaculates were tsRNAs and rsRNAs, both of which were positively correlated with sperm motility. Meanwhile, a high-sugar diet caused simultaneous changes in the contents of tsRNAs and rsRNAs [15]. These findings suggested that a high-sugar diet could affect sperm quality by altering rsRNA profiles, and thus rsRNAs might be an important clue linking obesity to male infertility.

In this study, apart from attenuating the chemoresistance of prostate cancer cells, rsRNA-28S also enhanced cellular proliferation (**Supplementary Fig. 5**). It has been reported that rsRNA-28S is involved in the regulation of metabolic pathways. Specifically, rsRNA-28S overexpression mediated the expression of gluconeogenic enzymes and peroxisome proliferator-activated receptor-γ (PPAR-γ) through regulating promoter activity, which in turn impinging on glucose and lipid metabolism. Additionally, rsRNA-28S reduced intracellular ATP levels and increased the phosphorylation levels of ERK1/2, p90RSK, Elk-1 and p70S6K [29]. Cancer is, in part, recognized as a kind of metabolic disease that exhibits deregulated cellular energetics [30,31]. Therefore, we may shed further light on the regulatory roles of rsRNAs in tumorigenesis by deciphering their effects on cellular metabolism.

The mechanism of action displayed by rsRNAs is similar to that of other sncRNAs. For example, rsRNAs interact with Ago, PIWI, or PHAS proteins, reflecting that rRNAs not only serve as a central player in the structured/function of translational machinery of the ribosome, but also give rise to functional rsRNAs that mediate gene expression at the post-transcriptional level. rsRNAs may function similar to miRNAs and target mRNAs to prevent their expression through inhibiting translation or inducing mRNA degradation. Alternatively, rsRNAs may act similar to piRNAs which bind DNA and prevent the translocation of transposons [28]. Current evidence indicate that a series of rsRNA-28S, of 20–22 nt in length, are asso-

ciated with Ago1 and Ago2 in various species, such as *Arabidopsis*, *Drosophila*, and human cell lines. This suggests that rsRNA-28S may exert their function via Ago complexes, just like miRNAs [32–34]. Notably, several noncanonical miRNAs indeed belong to rsRNA-28S such as mmu-miR-5102, mmu-miR-5105, mmu-miR-5109, and mmu-miR-5115, all of which map to rsRNA-28S [21,35]. Considering this, we speculated that rsRNA-28S in this study may target genes in a miRNA-like manner. The dual-luciferase reporter gene assay confirmed that rsRNA-28S inhibited the translation of *PTGIS* mRNA by directly targeting its 3′UTR (Fig. 4C,D). Moreover, rsRNA-28S inhibition increased the PTGIS expression level in prostate cancer cells (Fig. 4A), and PTGIS overexpression significantly enhanced cellular chemoresistance (Fig. 5). Together, these results strongly suggest that rsRNA-28S attenuated the chemoresistance of prostate cancer cells by downregulating its downstream target PTGIS transcript. As a member of the cytochrome P450 superfamily, PTGIS catalyzes the isomerization of prostaglandin H2 (PGH2) to prostaglandin I2 (PGI2). PGI2, also known as prostacyclin, is a potent mediator of vasodilation and an inhibitor of platelet aggregation [36]. PTGIS is often downregulated in several types of cancer, including lung cancer, colorectal cancer, and prostate cancer [37–39]. However, the expression level of PTGIS in hepatic metastases was noticeably higher than that measured in matched primary colon cancer tissues [40]. Furthermore, PTGIS was found to be an unfavorable prognostic indicator for lung cancer, ovarian cancer, and gastric cancer, with higher PTGIS expression levels indicating shorter overall survival time [41]. Moreover, residual cycling of PTGIS-positive CSCs was found to likely regenerate drug resistance to 5-Aza-dC and TSA in ovarian cancer cells [42]. Analogously, we found that PTGIS enhanced the chemoresistance of prostate cancer cells, although the underlying mechanism of this phenotype is currently unknown.

5. Conclusions

In conclusion, we have demonstrated that rsRNA-28S attenuates the chemoresistance of prostate cancer cells by downregulating its target transcript PTGIS. This finding supports the potential of rsRNA-28S in monitoring cancer therapy, prognostic prediction, and as a therapeutic target in prostate cancer.

Availability of Data and Materials

All data generated or analyzed during this study are included in this published article.

Author Contributions

YZ and YT designed the study. DQ and YLiu performed this study and wrote the draft of the manuscript. YZ, YLei, CZ and YB participated in the revision of draft and the interpretation of data for the work. All authors contributed to editorial changes in the manuscript. All authors read and approved the final manuscript. All authors have participated sufficiently in the work and agreed to be accountable for all aspects of the work.

Ethics Approval and Consent to Participate

The study was approved by the Ethics Committee of the First Affiliated Hospital of Chongqing Medical University (2021-759).

Acknowledgment

We are grateful to Prof Xinghuan Wang (Department of Urology, Zhongnan Hospital of Wuhan University) for endowing the PTGIS expression plasmid.

Funding

This study was supported by the National Natural Science Foundation of China (82173243, 81872014, 81672301), Scientific and Technological Research Projects of Chongqing Education Commission (KJQN202100403) and Chongqing Natural Science Foundation (CSTB2022NSCQ-MSX0123).

Conflict of Interest

The authors declare no conflict of interest.

Supplementary Material

Supplementary material associated with this article can be found, in the online version, at https://doi.org/10.31083/j.fbl2805102.

References

[1] Qiu H, Cao S, Xu R. Cancer incidence, mortality, and burden in China: a time-trend analysis and comparison with the United States and United Kingdom based on the global epidemiological data released in 2020. Cancer Communications. 2021; 41: 1037–1048.

[2] Feng RM, Zong YN, Cao SM, Xu RH. Current cancer situation in China: good or bad news from the 2018 Global Cancer Statistics? Cancer Communications. 2019; 39: 22.

[3] Chen W, Zheng R, Baade PD, Zhang S, Zeng H, Bray F, *et al*. Cancer statistics in China, 2015. CA: A Cancer Journal for Clinicians. 2016; 66: 115–132.

[4] Zheng R, Zhang S, Zeng H, Wang S, Sun K, Chen R, *et al*. Cancer incidence and mortality in China, 2016. Journal of the National Cancer Center. 2022; 2.

[5] Siegel RL, Miller KD, Fuchs HE, Jemal A. Cancer statistics, 2022. CA: A Cancer Journal for Clinicians. 2022; 72: 7–33.

[6] Karantanos T, Corn PG, Thompson TC. Prostate cancer progression after androgen deprivation therapy: mechanisms of castrate resistance and novel therapeutic approaches. Oncogene. 2013; 32: 5501–5511.

[7] Tannock IF, de Wit R, Berry WR, Horti J, Pluzanska A, Chi KN, *et al*. Docetaxel plus prednisone or mitoxantrone plus prednisone for advanced prostate cancer. The New England Journal of Medicine. 2004; 351: 1502–1512.

[8] Litwin MS, Tan HJ. The Diagnosis and Treatment of Prostate

Cancer: A Review. The Journal of the American Medical Association. 2017; 317: 2532–2542.
[9] Wade CA, Kyprianou N. Profiling Prostate Cancer Therapeutic Resistance. International Journal of Molecular Sciences. 2018; 19: 904.
[10] Lei X, Hu X, Zhang T, Zhang J, Wu C, Hong W, *et al*. HMGB1 release promotes paclitaxel resistance in castration-resistant prostate cancer cells via activating c-Myc expression. Cellular Signalling. 2020; 72: 109631.
[11] Hwang C. Overcoming docetaxel resistance in prostate cancer: a perspective review. Therapeutic Advances in Medical Oncology. 2012; 4: 329–340.
[12] Chen Q, Zhang X, Shi J, Yan M, Zhou T. Origins and evolving functionalities of tRNA-derived small RNAs. Trends in Biochemical Sciences. 2021; 46: 790–804.
[13] Shi J, Zhou T, Chen Q. Exploring the expanding universe of small RNAs. Nature Cell Biology. 2022; 24: 415–423.
[14] Chu C, Yu L, Wu B, Ma L, Gou LT, He M, *et al*. A sequence of 28S rRNA-derived small RNAs is enriched in mature sperm and various somatic tissues and possibly associates with inflammation. Journal of Molecular Cell Biology. 2017; 9: 256–259.
[15] Nätt D, Kugelberg U, Casas E, Nedstrand E, Zalavary S, Henriksson P, *et al*. Human sperm displays rapid responses to diet. PLoS Biology. 2019; 17: e3000559.
[16] Nätt D, Öst A. Male reproductive health and intergenerational metabolic responses from a small RNA perspective. Journal of Internal Medicine. 2020; 288: 305–320.
[17] Hua M, Liu W, Chen Y, Zhang F, Xu B, Liu S, *et al*. Identification of small non-coding RNAs as sperm quality biomarkers for in vitro fertilization. Cell Discovery. 2019; 5: 20.
[18] Zhang Y, Chen Q. The expanding repertoire of hereditary information carriers. Development. 2019; 146: dev170902.
[19] Chen Z, Sun Y, Yang X, Wu Z, Guo K, Niu X, *et al*. Two featured series of rRNA-derived RNA fragments (rRFs) constitute a novel class of small RNAs. PLoS ONE. 2017; 12: e0176458.
[20] Gu W, Shi J, Liu H, Zhang X, Zhou JJ, Li M, *et al*. Peripheral blood non-canonical small non-coding RNAs as novel biomarkers in lung cancer. Molecular Cancer. 2020; 19: 159.
[21] Shi J, Zhang Y, Tan D, Zhang X, Yan M, Zhang Y, *et al*. PANDORA-seq expands the repertoire of regulatory small RNAs by overcoming RNA modifications. Nature Cell Biology. 2021; 23: 424–436.
[22] Chen H, Li H, Chen Q. INPP4B reverses docetaxel resistance and epithelial-to-mesenchymal transition via the PI3K/Akt signaling pathway in prostate cancer. Biochemical and Biophysical Research Communications. 2016; 477: 467–472.
[23] Lu M, Ge Q, Wang G, Luo Y, Wang X, Jiang W, *et al*. CIRBP is a novel oncogene in human bladder cancer inducing expression of HIF-1α. Cell Death & Disease. 2018; 9: 1046.
[24] Ji Y, Xie M, Lan H, Zhang Y, Long Y, Weng H, *et al*. PRR11 is a novel gene implicated in cell cycle progression and lung cancer. The International Journal of Biochemistry & Cell Biology. 2013; 45: 645–656.
[25] Lorenz R, Bernhart SH, Höner Zu Siederdissen C, Tafer H, Flamm C, Stadler PF, *et al*. ViennaRNA Package 2.0. Algorithms for Molecular Biology. 2011; 6: 26.
[26] Nielsen CB, Shomron N, Sandberg R, Hornstein E, Kitzman J, Burge CB. Determinants of targeting by endogenous and exogenous microRNAs and siRNAs. RNA. 2007; 13: 1894–1910.
[27] Shibue T, Weinberg RA. EMT, CSCs, and drug resistance: the mechanistic link and clinical implications. Nature Reviews. Clinical Oncology. 2017; 14: 611–629.
[28] Lambert M, Benmoussa A, Provost P. Small Non-Coding RNAs Derived From Eukaryotic Ribosomal RNA. Non-Coding RNA. 2019; 5: 16.
[29] Wei H, Zhou B, Zhang F, Tu Y, Hu Y, Zhang B, *et al*. Profiling and identification of small rDNA-derived RNAs and their potential biological functions. PLoS ONE. 2013; 8: e56842.
[30] Hanahan D. Hallmarks of Cancer: New Dimensions. Cancer Discovery. 2022; 12: 31–46.
[31] Hanahan D, Weinberg RA. Hallmarks of cancer: the next generation. Cell. 2011; 144: 646–674.
[32] Benhamed M, Herbig U, Ye T, Dejean A, Bischof O. Senescence is an endogenous trigger for microRNA-directed transcriptional gene silencing in human cells. Nature Cell Biology. 2012; 14: 266–275.
[33] Czech B, Malone CD, Zhou R, Stark A, Schlingeheyde C, Dus M, *et al*. An endogenous small interfering RNA pathway in Drosophila. Nature. 2008; 453: 798–802.
[34] Zhang X, Zhao H, Gao S, Wang WC, Katiyar-Agarwal S, Huang HD, *et al*. Arabidopsis Argonaute 2 regulates innate immunity via miRNA393(*)-mediated silencing of a Golgi-localized SNARE gene, MEMB12. Molecular Cell. 2011; 42: 356–366.
[35] Castellano L, Stebbing J. Deep sequencing of small RNAs identifies canonical and non-canonical miRNA and endogenous siRNAs in mammalian somatic tissues. Nucleic Acids Research. 2013; 41: 3339–3351.
[36] Ershov PV, Mezentsev YV, Kopylov AT, Yablokov EO, Svirid AV, Lushchyk AY, *et al*. Affinity Isolation and Mass Spectrometry Identification of Prostacyclin Synthase (PTGIS) Subinteractome. Biology. 2019; 8: 49.
[37] Cathcart MC, Gray SG, Baird AM, Boyle E, Gately K, Kay E, *et al*. Prostacyclin synthase expression and epigenetic regulation in nonsmall cell lung cancer. Cancer. 2011; 117: 5121–5132.
[38] Frigola J, Muñoz M, Clark SJ, Moreno V, Capellà G, Peinado MA. Hypermethylation of the prostacyclin synthase (PTGIS) promoter is a frequent event in colorectal cancer and associated with aneuploidy. Oncogene. 2005; 24: 7320–7326.
[39] Kwon OK, Ha YS, Na AY, Chun SY, Kwon TG, Lee JN, *et al*. Identification of Novel Prognosis and Prediction Markers in Advanced Prostate Cancer Tissues Based on Quantitative Proteomics. Cancer Genomics & Proteomics. 2020; 17: 195–208.
[40] Lichao S, Liang P, Chunguang G, Fang L, Zhihua Y, Yuliang R. Overexpression of PTGIS could predict liver metastasis and is correlated with poor prognosis in colon cancer patients. Pathology Oncology Research. 2012; 18: 563–569.
[41] Dai D, Chen B, Feng Y, Wang W, Jiang Y, Huang H, *et al*. Prognostic value of prostaglandin I2 synthase and its correlation with tumor-infiltrating immune cells in lung cancer, ovarian cancer, and gastric cancer. Aging. 2020; 12: 9658–9685.
[42] Singh AK, Chandra N, Bapat SA. Evaluation of Epigenetic Drug Targeting of Heterogenous Tumor Cell Fractions Using Potential Biomarkers of Response in Ovarian Cancer. Clinical Cancer Research. 2015; 21: 5151–5163.